

Text-driven 3D Human Generation via Contrastive Preference Optimization

Pengfei Zhou, Xukun Shen, Yong Hu

Abstract—Recent advances in Score Distillation Sampling (SDS) have improved 3D human generation from textual descriptions. However, existing methods still face challenges in accurately aligning 3D models with long and complex textual inputs. To address this challenge, we propose a novel framework that introduces contrastive preferences, where human-level preference models, guided by both positive and negative prompts, assist SDS for improved alignment. Specifically, we design a preference optimization module that integrates multiple models to comprehensively capture the full range of textual features. Furthermore, we introduce a negation preference module to mitigate over-optimization of irrelevant details by leveraging static-dynamic negation prompts, effectively preventing “reward hacking”. Extensive experiments demonstrate that our method achieves state-of-the-art results, significantly enhancing texture realism and visual alignment with textual descriptions, particularly for long and complex inputs.

Index Terms—3D Human Generation, Text-driven, Score Distillation Sampling, Human Preferences.

I. INTRODUCTION

The creation of high-fidelity 3D human models from detailed textual descriptions has attracted widespread attention in the industry, with applications spanning VR/AR, filmmaking, animation production, the metaverse, and more. Traditional methods for customizing personalized avatars are time-consuming and labor-intensive. With the development of generative models, generative adversarial networks (GANs) and diffusion models have demonstrated the ability to generate realistic 2D images. However, when extending these techniques to 3D asset generation, challenges such as insufficient datasets and limited training resources arise. To address these issues, DreamFusion [1] introduces score distillation sampling (SDS) to leverage 2D prior knowledge from images for distilling 3D representations. This method produces reasonable results for single objects but struggles to model complex human bodies, resulting in problems such as Janus artifacts, geometric inconsistencies, over-saturation, and blurriness.

Several approaches [2], [4], [5] combine SDS with the SMPL-X [6] model to mitigate Janus artifacts and geometric inconsistencies. For example, TADA [4] proposes a subdivided SMPL-X to replace implicit representations, achieving high-quality 3D human generation. DreamWalta [5] utilizes ControlNet and SMPL-X to provide skeletal viewpoint-consistent 2D human guidance to resolve 3D geometric consistency issues. HumanGuassian [7] uses 3D Gaussian Splatting [8] (3DGS) and SMPL-X to represent 3D humans, collecting dense points from SMPL-X as initial point clouds for generating high-quality 3D human models. These methods leverage the SMPL-X as a prior for human representations, effectively

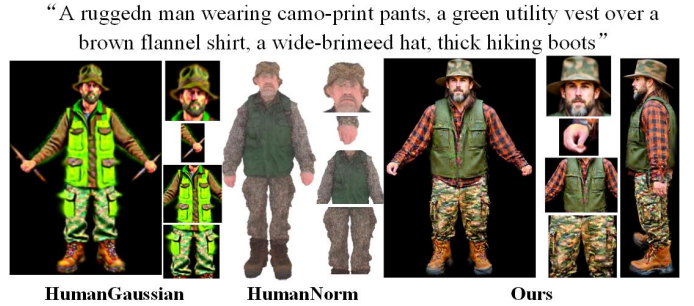


Fig. 1. Comparison of Long-Text 3D Human Generation Methods. We compare the state-of-the-art methods, HumanGaussian [2] and HumanNorm [3], for generating 3D humans from complex long-text descriptions. The results show that these methods struggle with full alignment, with elements such as the green vest and brown shirt being obscured by other colors. This issue arises due to the limited ability of SDS to disentangle complex textual features, leading to incomplete alignment with the long-text description.

mitigating issues such as multi-view inconsistencies. However, these methods struggle with aligning long text descriptions and often overlook certain word attributes, such as color, type, and objects. As shown in Fig. 1, a green vest was replaced with a neon green vest, and a brown flannel shirt was substituted with a camouflage shirt.

The underlying reasons for these issues are as follows: SDS fails to decouple word attributes at a fine-grained level, which leads to certain attributes, such as “color” or “object,” being overshadowed by more prominent features in the text, thereby distorting the intended description. In addition, generating a realistic and text-aligned human body with fine-grained disentangled 3D avatars remains a significant challenge.

In this paper, we propose a novel framework to address the weak alignment capabilities of existing methods when dealing with long texts. The core of our approach is the introduction of contrastive preferences, which enhances the alignment between long textual descriptions and 3D human models. Specifically, we introduce a preference optimization module that integrates multiple preference models, allowing the model to capture semantic information from different segments of a long text. This fine-grained disentanglement of textual attributes improves the model’s ability to align with long texts more accurately. We utilize a combination of ImageReward [9], PickScore [10], and HPS_V2 [11] preference models to evaluate the alignment between long texts and the generated 3D models. The integration of these models enables complementary perception of the semantic nuances within the text, leading to enhanced alignment precision. Therefore,

the reward gradients generated by the preference optimization module enhance the unoptimized textual information during the SDS process, improving the 3D representation and boosting long-text alignment.

However, preference models can often lead to the "reward hacking" problem, where excessive optimization of the 3D Gaussian representation results in the generation of irrelevant objects, thereby producing unrealistic outputs. To address this issue, we propose a negation preference optimization module that introduces negation prompts as additional constraints. These negation prompts consist of static negation prompts (e.g., "blurry," "low contrast," "JPEG artifacts") as well as dynamic negation prompts. The dynamic negation prompts are generated by reordering the word attributes in the long text descriptions to create further negation prompts (e.g., changing "white canvas shoes, red jacket" to "red canvas shoes, white jacket"). This strategy helps ensure that the model does not excessively focus on specific attributes at the expense of others, leading to more balanced and realistic 3D outputs. Our contributions are summarized as follows:

- First, we introduce the preference optimization module, which integrates multiple preference models to fine-grain the semantic disentangling of each segment of the text. This improves the overall alignment between long texts and the generated 3D human models by capturing the detailed semantics of short text segments more effectively.
- Additionally, we propose a negation preference optimization module. This module incorporates both static and dynamic negation prompts to constrain the preference models, preventing the generation of irrelevant objects.
- Finally, extensive quantitative experiments demonstrate that our method outperforms recent approaches in terms of textual alignment accuracy. Qualitative results further show that our method achieves superior visual quality, generating more semantically accurate and visually coherent 3D models compared to existing methods.

II. RELATED WORK

A. Text-to-3D Generation

With the remarkable advancements in text-to-image generation models, there has been an increasing interest among researchers in extending this technology to the realm of text-to-3D generation [1], [12], [13]. Early approaches [14], [15] employed CLIP loss functions to supervise 3D representations, which yielded promising results. However, these methods often resulted in 3D models that lacked realism and fine geometric details. A landmark study, DreamFusion, revolutionized this approach by replacing the CLIP model with a text-to-image diffusion model and introducing score distillation sampling (SDS) to optimize NeRF-based 3D representations. This innovative approach has since inspired several variants. ProlificDreamer [13] addresses the challenges of over-saturation and over-smoothing by introducing a variational SDS objective. Fantasia3D [12] introduces a novel decoupling strategy for geometry and appearance modeling,

utilizing SDS loss to optimize surface normals independently. More recently, DreamGaussian [7] replaces the NeRF-based representation with 3DGS, leading to significant reductions in runtime. Despite these advancements, however, these methods still face significant challenges in generating high-quality 3D human models, often resulting in Janus artifacts and geometric inconsistencies.

B. Text-driven 3D Human Generation

AvatarCLIP [14] integrates SMPL and Neus to generate 3D human avatars, using CLIP for supervision. However, it often produces 3D avatars that lack realism and are overly simplified. DreamAvatar [16] and AvatarCraft [15] leverage the SMPL model's pose and shape as priors for human body generation, but they frequently result in blurry 3D avatars. GAvatar [17] presents a novel implicit mesh learning method for capturing fine facial geometries and extracting detailed meshes. This method allows large-scale generation of animatable avatars using only text prompts.

Recently, some fine-tuned text-to-image methods have been introduced to improve the quality of text-driven 3D human generation. For example, HumanNorm [3] fine-tunes a text-to-image model to directly generate normal and depth maps from input text. The improved model is then used to optimize the avatar's geometry with SDS loss, and texture optimization is achieved through normal-conditioned ControNet. While these methods utilize various representations and fine-tune text-to-image models to achieve reasonable results, they fail to address the alignment of long texts, which makes it difficult to perfectly align the generated outputs with lengthy descriptions. To address this limitation, we propose a novel framework designed to improve the alignment capability for long texts.

C. Text-to-Image Generative Models Alignment

Existing text-to-image generation models are capable of producing high-quality 2D images; however, these generated images do not always align well with human preferences. As a result, alignment in the context of diffusion models has garnered increasing attention. Many approaches [9]–[11], [18] have focused on building large-scale text-image preference datasets and fine-tuning visual models as evaluation functions to enhance the alignment of generated images with human preferences. For example, ImageReward [9] proposes a reward-feedback learning method to optimize diffusion models, improving their alignment with human preferences. It also introduces the first universal text-image human preference reward model that effectively encodes human preferences. PickScore [10] constructs a large-scale open dataset for text-to-image generation, where fine-tuned CLIP better aligns with human preferences. HPS_V2 [11] presents a large-scale preference dataset, with curated text prompts and images intentionally collected to minimize potential bias. LongAlign [19] proposes a segment-level encoding method for handling long texts and a decomposed preference optimization approach for efficient alignment training. The method introduces a CLIP-based DenseScore preference model to enhance the alignment

of long texts. Our method combines multiple preference models to decouple short-text word attributes and enhance the alignment of long-text descriptions.

III. METHODOLOGY

Previous methods for text-to-3D human generation have struggled to effectively align long textual descriptions with 3D models. A primary limitation arises during the SDS optimization process, where models often converge to local optima, preventing the full optimization of all textual attributes. To address these challenges, we propose a novel framework that introduces contrastive preferences to enhance the alignment between long textual descriptions and 3D human models.

In Fig. 2, our pipeline consists of three key components: First, we utilize 3DGS and SMPL-X to represent the 3D human body, and we introduce the optimization paradigm for SDS to refine the 3D Gaussian representation in Sec. III-A. Second, we introduce the preference optimization module, which leverages multiple preference models to capture the semantic attributes of short texts, disentangle textual features, and enhance the optimization of neglected short-text features, thus improving the alignment as detailed in Sec. III-B. Additional, we propose the negation preference optimization module, which incorporates additional static-dynamic combined negation prompts to alleviate the generation of irrelevant objects caused by over-optimization of the preference models and improve texture clarity, as discussed in Sec. III-C.

A. Preliminaries

SMPL-X is a 3D parametric model used for modeling human body shape, encompassing the topology of the body, hands, and face. The model consists of 10,475 vertices and 54 keypoints. By combining pose parameters θ (which include body pose θ_b , facial pose θ_f , and finger pose θ_h), shape parameters β , and expression parameters Ψ , we can represent the 3D SMPL-X human model as $M(\beta, \theta, \Psi)$:

$$T(\beta, \theta, \Psi) = \bar{T} + B_s(\beta) + B_p(\theta) + B_e(\Psi), \quad (1)$$

$$M(\beta, \theta, \Psi) = LBS(T(\beta, \theta, \Psi), J(\beta), \theta, \omega), \quad (2)$$

where \bar{T} represents the average shape; B_s , B_p and B_e are the blending shape functions for shape, pose, and expression, respectively. $T(\beta, \theta, \Psi)$ is a non-rigid deformation starting from \bar{T} . The function $LBS(\cdot)$ is the linear blend skinning function, which transforms $T(\beta, \theta, \Psi)$ into the target pose θ . It defines the skeletal joints $J(\beta)$ and blending weights Ψ for each vertex.

Score Distillation Sampling to extract the 2D pre-trained diffusion prior for optimizing the 3D representation, we represent a 3D scene with θ and use a differentiable rendering function $g(\cdot)$ to obtain an image $x = g(\theta)$. By pushing the samples towards the denser regions of the real data distribution across all noise levels, we ensure that the rendering from each camera view closely resembles reasonable samples ϕ derived from the guidance diffusion model. In practice, DreamFusion employs Imagen as the score estimation function $\varepsilon_\phi(x_t, y)$, which predicts the sampling noise given a noisy image x_t , a

text embedding y , and a time step t . SDS then optimizes the 3D scene using gradient descent on θ :

$$\nabla_\theta L_{sds} = E_{\varepsilon, t} [\omega_t(\varepsilon_\phi(x_t; y) - \varepsilon) \frac{\partial x}{\partial \theta}], \quad (3)$$

We adopt the conventional SDS paradigm to optimize the 3D Gaussian representation. Instead of using random noise, we employ fixable noise, which enables the generation of more stable 3D human models. This modification enhances the robustness of the optimization process, ensuring that the generated 3D bodies are more consistent and accurate.

3D Gaussian Splatting provides an efficient representation for novel view synthesis and 3D reconstruction. Unlike implicit methods such as NeRF, 3D Gaussian Splatting represents the underlying scene using a set of anisotropic Gaussian functions. The parameters of these functions include the center position $\mu \in \mathbb{R}^3$, covariance $\Sigma \in \mathbb{R}^7$, color $c \in \mathbb{R}^3$, and opacity $\alpha \in \mathbb{R}$. By projecting the 3D Gaussian functions onto the camera's imaging plane, 2D Gaussian functions are assigned to corresponding tiles for point-based rendering:

$$G(p, \mu_i, \Sigma_i) = \exp(-\frac{1}{2}(p - \mu_i)), \quad (4)$$

$$c(p) = \sum_{i \in N} c_i \sigma_i \prod_{j=1}^{i-1} (1 - \sigma_j), \sigma_i = \alpha_i G(p, \mu_i, \Sigma_i), \quad (5)$$

where p represents the query point's position; μ_i , Σ_i , c_i , α_i and σ_i , are the center position, covariance, color, opacity, and density of the i -th Gaussian distribution, respectively. $G(p, \mu_i, \Sigma_i)$ is the value of the i -th Gaussian function at point p . N denotes the set of 3D Gaussians within the tile. Additionally, 3D Gaussian Splatting improves the GPU rasterization process, resulting in better quality, faster rendering speed, and lower memory usage.

B. Preference Optimization Module (POM)

We integrate multiple preference models, including ImageReward (IR), PickScore (PS), and HPS_V2 (HV), to leverage their complementary strengths in capturing the semantic properties of individual words and phrases within long textual descriptions. This multi-preference approach mitigates inconsistencies that often arise during the optimization process, enabling the model to more effectively perceive and align with the semantic nuances of complex texts.

By enhancing the model's comprehension of long-text inputs, our method improves the Gaussian distillation process within SDS. This leads to finer control over the resulting 3D representation, ensuring that all semantic attributes are effectively captured and accurately reflected in the generated 3D human models. The enhanced alignment enables the output 3D humans to faithfully embody the full range of characteristics described in the input text, achieving higher precision and realism.

Given the preference models $P = \{IR, PS, HV\}$, the long text $Y = \{y_1, y_2, \dots, y_k\}$, and the rendered image X , we first apply the proposed modules to obtain the preference scores $\{IR(X, Y), PS(X, Y), HV(X, Y)\}$. Then, we integrate the

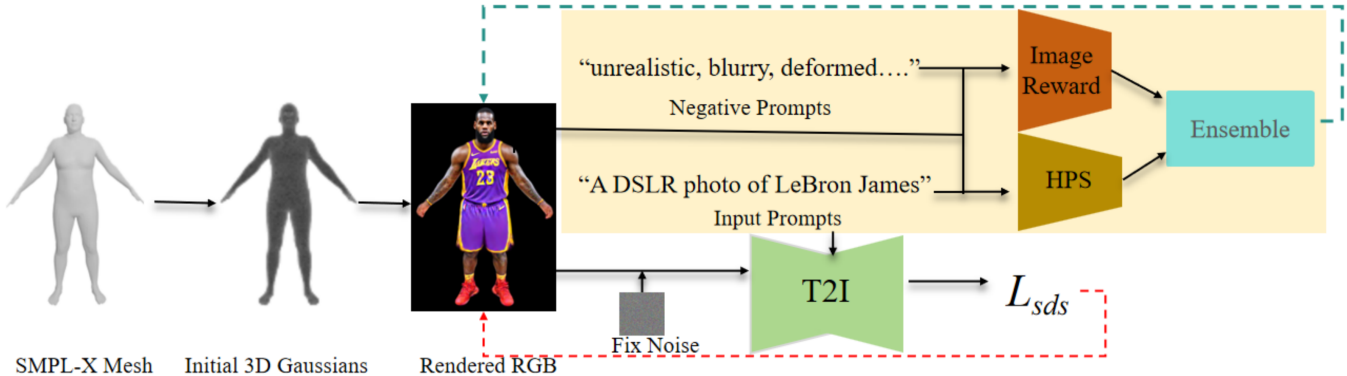


Fig. 2. Overview of the proposed Framework. We employ the neural representation of 3DGS to generate accurate 3D human models from long textual prompts. The process begins with sampling Gaussian functions densely on the surface of the SMPL-X human mesh, which serves as the initial centroid for model generation. To enhance the alignment between the long text and the 3D human model, we propose a preference optimization module. This module integrates preference models such as ImageReward and HPS_V2, which help to perceive the semantic nuances within each short text segment, improving overall alignment accuracy. Additionally, we introduce a negation preference optimization module, which incorporates both static and dynamic negation prompts to prevent over-optimization in the preference models. These negation prompts ensure that the models do not overly emphasize certain attributes at the cost of others. The entire framework primarily relies on SDS, where the preference models assist in refining the SDS process, thereby enhancing the alignment capability of long texts with 3D human representations.

semantic information of the short texts in the long text by employing a simple weighted summation method, which enhances the alignment of the long text. The preference function can be represented as:

$$C_+^p = \frac{1}{N} \sum_{i=0}^{N=2} \lambda_i P_i(X, Y), \quad (6)$$

where N is the number of preference models, and λ_i represents the weight of the i -th preference model.

C. Negative Preference Optimization Module (NPOM)

To prevent the preference model from overfitting and deviating from the intended optimization direction, we introduce a contrastive approach to constrain the model. To more effectively prevent the occurrence of “reward collapse,” we construct a comprehensive negation prompt. The negation prompt consists of two components. The first component is a fixed set of negation words, similar to the negative prompts used in diffusion models. We define the static negation prompt as $\text{static_neg_prompt} = \{\text{'blurry, oversaturated, noisy, ..., jpeg artifacts'}\}$. The second component involves dynamic negation prompt, where we dynamically rearrange the words and potentially related objects in the prompt to avoid unreasonable situations. For example, if the prompt states, “a person is wearing a white jacket and black pants,” we can dynamically restructure it into $\text{dyn_neg_prompt} = \{\text{'wearing a black jacket, white pants'}\}$.

Given the negation prompt Y_{neg} , we apply the proposed model to obtain the negation preference scores $\text{IR}(X, Y_{\text{neg}})$, $\text{PS}(X, Y_{\text{neg}})$. Subsequently, we use the averaged negation preference scores to constrain the preference model and prevent overfitting. The negation preference function can be defined as:

$$C_-^p = \frac{1}{N} \sum_{i=1}^{N=2} P_i(X, Y_{\text{neg}}), \quad (7)$$

IV. EXPERIMENTS

A. Experiment Setups

Training and 3D GS Setups. The 3D Gaussian model is initialized with 100k instances, uniformly sampled on the surface of the SMPL-X mesh with an opacity of 0.1. The entire 3DGS training process requires 3600 iterations, with dense sampling and pruning performed every 300 steps, ranging from 300 to 2100 iterations. The pruning phase is conducted with a threshold factor of 0.008, applied every 300 steps from iteration 2400 to 3300. The overall framework is trained using the Adam optimizer with β values of [0.9, 0.99]. The learning rates for the center position μ , scale factor s , rotation quaternion q , color c , and opacity α are set to 5×10^{-5} , 1×10^{-3} , 1×10^{-2} , 1.25×10^{-2} , and 1×10^{-2} , respectively.

Implementation details. Our method is implemented within the ThreeStudio framework in PyTorch. We employ the Adam optimizer with a learning rate of 0.001. The camera’s distance is constrained within the range [1.5, 2.0], the field of view (fovy) within [40°, 70°], the height within [-30°, 30°], and the azimuth within [-180°, 180°]. The SDS loss weight is set to 1. The preference model weights are set to $\lambda_1 = 20$, $\lambda_2 = 15$, $\lambda_3 = 10$. We set the guidance scale as 7.5 and sample time steps $t \sim U(0.02, 0.50)$. We use a training resolution of 1024 and a batch size of 4. The entire optimization process takes 0.8 hours on a single NVIDIA RTX 4090 GPU.

Baselines. We compare our approach with state-of-the-art (SOTA) methods for generating 3D human bodies from complex text. The compared text-to-3D human methods include TADA [4], HumanGaussian [2], and HumanNorm [3].

Long-text dataset construction. We randomly generate 30 textual descriptions of dressed characters using ChatGPT-01, with each example consisting of a top, bottom, and two other random accessories. The 30 human clothing descriptions are used to evaluate 3D human body generation.

B. Qualitative Evaluations

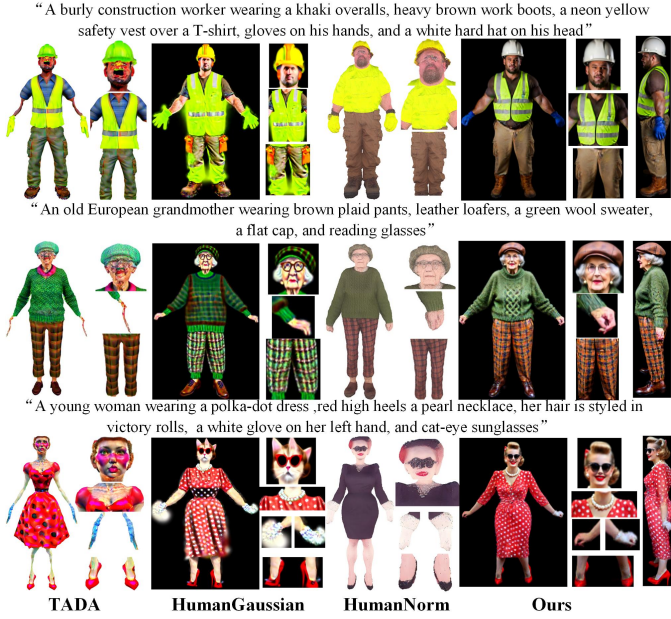


Fig. 3. Qualitative comparisons with the SOTA methods.

We conduct a qualitative comparison with recent methods on complex long-text descriptions, focusing on the alignment of accessory color, position, and type. As shown in Fig. 3, our method achieves superior alignment across these aspects. For example, it accurately generates “a white safety helmet and khaki overalls” in the first image and “brown plaid pants” in the second, demonstrating precise color rendering. Additionally, our method correctly places “white gloves on the left hand” in the third example, addressing positional constraints effectively. Furthermore, it captures fine-grained accessory details such as “a polka-dot dress, pearl necklace, victory rolls hairstyle, and cat-eye sunglasses,” showcasing its ability to align complex accessory types with textual descriptions.

In contrast, existing methods struggle with these aspects, particularly failing to align spatial details like “a white glove on the left hand” and “a white safety helmet.” To overcome this limitation, we introduce negative prompts in the preference module, such as “wearing a white glove on the right hand” and “wearing a yellow safety helmet,” which impose explicit constraints to guide the generation process.

Overall, these results demonstrate that our method effectively achieves fine-grained semantic alignment with textual descriptions, significantly improving visual fidelity and consistency in complex multi-attribute texts.

C. Quantitative Evaluation

Quantitatively evaluating the quality of generated 3D human models remains a significant challenge, as user studies often suffer from subjective biases due to participant variability. To address this issue, we introduce DenseScore [19], a preference model built upon CLIP and fine-tuned on a large-scale

TABLE I
QUANTITATIVE COMPARISONS WITH TEXT-TO-3D HUMAN METHODS

| Method | CLIP Score (\uparrow) | DenseScore Score (\uparrow) |
|-----------------|---------------------------|---------------------------------|
| TADA | 29.16 | 24.93 |
| HumanGaussian | 30.67 | 27.68 |
| HumanNorm | 30.48 | 27.72 |
| Ours (w/o POM) | 30.15 | 28.84 |
| Ours (w/o NPOM) | 30.98 | 30.65 |
| Ours | 32.09 | 32.47 |

preference dataset. DenseScore serves as an aesthetic evaluation framework that significantly improves the assessment of alignment between complex textual descriptions and the corresponding rendered images. Compared to previous preference models, DenseScore demonstrates superior performance in evaluating fine-grained semantic and visual consistency, particularly for complex multi-attribute prompts.

Additionally, we employ the CLIP Score to evaluate the semantic alignment between the generated 3D models and long-text descriptions, where higher scores denote improved consistency. As shown in Tab. I, our method achieves superior DenseScore scores, indicating that the rendered multi-view images of our 3D human models better conform to human aesthetic preferences. Simultaneously, the high CLIP scores demonstrate strong alignment between the generated views and the input textual descriptions. These results underscore the effectiveness of our approach in generating 3D human models with both high aesthetic quality and semantic fidelity. Finally, we provide detailed results of the user study in the supplementary materials.

D. Ablation Study

Effect of Preference Optimization Module. In Fig. 4 (c), we introduce the Preference Optimization Model (POM) to evaluate its effectiveness in improving the alignment with long-text descriptions. The results demonstrate that POM significantly enhances the generation quality, particularly for complex prompts.

For instance, in the first example, the generated textures clearly exhibit a camouflage top and a multi-functional belt loaded with gear and ammunition, as described. In the second example, the model successfully renders fine-grained details, such as cat-eye glasses and gloves. In Tab. I, removing POM results in a significant drop in both the CLIP score and the DenseScore score. These observations confirm that the inclusion of POM greatly improves alignment with complex textual descriptions, while also exhibiting strong robustness in handling intricate visual attributes.

Effect of Negative Preference Optimization Module. In Fig. 4 (b) - (d), we observe that introducing POM can occasionally lead to over-optimization, resulting in unintended artifacts. For instance, in the first example, a gun appears despite being unrelated to the prompt, and in the second example, a glove is generated on the right hand, which was not described.

"A man wearing a full camouflage fatigues, sturdy tactical boots, kevlar vest with a helmet, and a utility belt filled gear and ammunition"



"A young woman wearing a polka-dot dress, red high heels, a pearl necklace, her hair is styled in victory rolls, a white glove on her left hand, and cat-eye sunglasses"

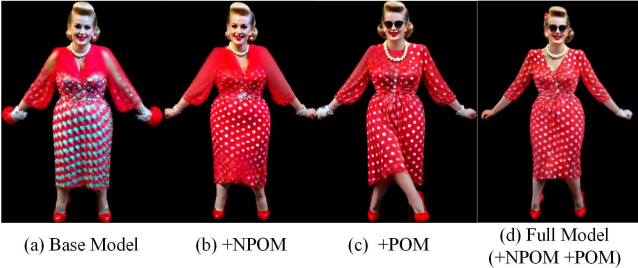


Fig. 4. Ablation study of our method. We present the results of frontal human view generation under two ablation settings to better visualize and compare: (a) Base model; (b) +NPOM; (c) +POM; and (d) Full model.

To address this issue, we introduce the Negative Preference Model (NPOM), which mitigates over-optimization by incorporating negative prompts. Specifically: In Fig. 4 (b) demonstrates that introducing static negative prompts significantly improves the clarity and realism of 3D human textures, enhancing their visual fidelity. In Fig. 4 (d) shows that incorporating dynamic negative prompts effectively eliminates the artifacts introduced by POM, such as irrelevant objects. In Tab. I, removing NPOM leads to a decline in both CLIP scores and DenseScore, highlighting its importance. In summary, NPOM effectively alleviates over-optimization, ensuring accurate, artifact-free 3D human model generation with improved visual fidelity and semantic alignment.

V. CONCLUSION

In this paper, we propose a novel framework to improve the alignment of 3D human generation from long textual descriptions, addressing the limitations of current methods. Our approach introduces contrastive preferences, leveraging human-level preference models with both positive and negative prompts to guide SDS for better alignment. We present a preference optimization module that integrates multiple complementary models, enabling the capture of a wider range of textual features, thereby enhancing alignment accuracy. Additionally, we introduce a negation preference module to prevent over-optimization of irrelevant features. Experimental results demonstrate that our method significantly outperforms existing approaches in terms of both texture realism and visual alignment with textual descriptions.

In the future, we plan to address challenges such as over-saturation and fuzziness within SDS. By refining how SDS

handles these issues, we aim to further enhance the accuracy and robustness of 3D human generation from complex and diverse textual inputs.

APPENDIX

User Study. To further evaluate and validate the quality of the generated 3D human models, we conducted an additional user study designed to ensure a fair and comprehensive comparison with existing methods. Specifically, we utilized ChatGPT to randomly generate a set of 30 prompts, comprising 15 long-text descriptions (complex multi-attribute prompts) and 15 simple-text descriptions (basic attribute prompts). This balanced combination allowed us to assess performance under both simple and complex textual conditions.

A total of 20 participants were recruited to perform a subjective evaluation of the generated 3D models. Each participant was presented with the rendered 3D human outputs from different methods and asked to score them based on the following two key criteria: Texture Quality, Geometry Quality. Participants assigned scores on a scale of 1 to 10, where a higher score indicates better performance in the respective evaluation aspect.

The evaluation results are presented in Tab. II. Notably, our method consistently outperformed all competing approaches across all three evaluation metrics. In particular, our method achieved superior texture quality, accurately rendered fine-grained geometry, and demonstrated strong text alignment under both simple and complex prompts. These findings underscore the robustness and effectiveness of our method in generating high-quality 3D human models that align closely with user expectations and textual descriptions.

This user study provides additional evidence of the practical advantages of our approach and highlights its ability to handle complex multi-attribute scenarios while maintaining superior visual fidelity and semantic consistency.

TABLE II
QUANTITATIVE COMPARISONS WITH TEXT-TO-3D HUMAN METHODS

| Method | Texture Quality (\uparrow) | Geometry Quality (\uparrow) |
|---------------|--------------------------------|---------------------------------|
| TADA | 6.5 | 7.4 |
| HumanGaussian | 8.3 | 7.6 |
| HumanNorm | 8.2 | 7.9 |
| Ours | 8.4 | 8.0 |

A. Qualitative Evaluations

In Fig.6, we present an extensive set of experimental results, conducting comparisons against two alternative methods to validate the robustness and effectiveness of our proposed approach. Specifically, we evaluate our approach on a diverse set of complex long-text descriptions containing intricate and fine-grained attributes, such as color, object types, and stylistic details. By including text prompts of varying complexity, we ensure a comprehensive assessment of our method's alignment capability under different scenarios.

The results demonstrate that our method consistently achieves superior performance in generating 3D human models that accurately align with the provided textual descriptions, even as the text complexity increases. Notably, our framework effectively captures nuanced textual attributes and avoids common artifacts observed in previous methods, such as geometric inconsistencies and attribute misalignments. These findings further underscore the robustness and generalization capability of our approach across varying levels of textual complexity, establishing its effectiveness in handling both simple and highly detailed long-text prompts.

B. Applications

Text-based Editing. Our method offers the ability to edit the texture of the generated 3D human models by adjusting the input textual prompts. This feature enables fine-grained control over attributes such as clothing color, style, and hairstyle, providing a versatile editing mechanism. As illustrated in Fig. 5 (a), we demonstrate this capability by modifying the color and style of Curry's clothing, as well as his hairstyle.

These results highlight the flexibility of our approach in generating personalized and diverse 3D human models while maintaining high visual quality and alignment with the modified prompts. This editing capability is particularly valuable for applications requiring dynamic adjustments, such as content creation, virtual avatars, and digital entertainment.

Text-based Style Creation. Our method also enables the generation of 3D human models in diverse styles by introducing specific style types into the input textual prompts. This feature allows for precise control over the stylistic attributes of the generated models, such as color schemes and visual styles. As shown in Fig. 5 (b), we demonstrate this capability by modifying man's style and color, effectively altering the overall appearance of the generated 3D human model.

This flexibility underscores the adaptability of our approach, allowing users to seamlessly incorporate different stylistic preferences into the generation process. Such a capability is particularly beneficial for applications involving virtual avatars, fashion design, and digital content creation, where style customization is essential.

REFERENCES

- [1] Ben Poole, Ajay Jain, Jonathan T. Barron, and Ben Mildenhall, "Dreamfusion: Text-to-3d using 2d diffusion," *ArXiv*, vol. abs/2209.14988, 2022.
- [2] Xian Liu, Xiaohang Zhan, Jiaxiang Tang, Ying Shan, Gang Zeng, Dahua Lin, Xihui Liu, and Ziwei Liu, "Humangaussian: Text-driven 3d human generation with gaussian splatting," in *2024 IEEE/CVF Conference on Computer Vision and Pattern Recognition (CVPR)*, 2024, pp. 6646–6657.
- [3] Xin Huang, Ruizhi Shao, Qi Zhang, Hongwen Zhang, Ying Feng, Yebin Liu, and Qing Wang, "Humannorm: Learning normal diffusion model for high-quality and realistic 3d human generation," in *2024 IEEE/CVF Conference on Computer Vision and Pattern Recognition (CVPR)*, 2024, pp. 4568–4577.
- [4] Tingting Liao, Hongwei Yi, Yuliang Xiu, Jiaxiang Tang, Yangyi Huang, Justus Thies, and Michael J. Black, "Tada! text to animatable digital avatars," in *2024 International Conference on 3D Vision (3DV)*, 2024, pp. 1508–1519.
- [5] Yukun Huang, Jianan Wang, Ailing Zeng, He Cao, Xianbiao Qi, Yukai Shi, Zheng-Jun Zha, and Lei Zhang, "DreamWaltz: Make a Scene with Complex 3D Animatable Avatars," in *Advances in Neural Information Processing Systems*, 2023.
- [6] Matthew Loper, Naureen Mahmood, Javier Romero, Gerard Pons-Moll, and Michael J. Black, "Smpl: a skinned multi-person linear model," *ACM Trans. Graph.*, vol. 34, no. 6, Oct. 2015.
- [7] Jiaxiang Tang, Jiawei Ren, Hang Zhou, Ziwei Liu, and Gang Zeng, "Dreamgaussian: Generative gaussian splatting for efficient 3d content creation," *arXiv preprint arXiv:2309.16653*, 2023.
- [8] Keyang Ye, Qiming Hou, and Kun Zhou, "3d gaussian splatting with deferred reflection," in *ACM SIGGRAPH 2024 Conference Papers*, New York, NY, USA, 2024, *SIGGRAPH '24*, Association for Computing Machinery.
- [9] Jiazheng Xu, Xiao Liu, Yuchen Wu, Yuxuan Tong, Qinkai Li, Ming Ding, Jie Tang, and Yuxiao Dong, "Imagereward: Learning and evaluating human preferences for text-to-image generation," 2023.
- [10] Yuval Kirstain, Adam Polyak, Uriel Singer, Shahbuland Matiana, Joe Penna, and Omer Levy, "Pick-a-pic: An open dataset of user preferences for text-to-image generation," 2023.
- [11] Xiaoshi Wu, Yiming Hao, Keqiang Sun, Yixiong Chen, Feng Zhu, Rui Zhao, and Hongsheng Li, "Human preference score v2: A solid benchmark for evaluating human preferences of text-to-image synthesis," *arXiv preprint arXiv:2306.09341*, 2023.
- [12] Rui Chen, Yongwei Chen, Ningxin Jiao, and Kui Jia, "Fantasia3d: Disentangling geometry and appearance for high-quality text-to-3d content creation," in *2023 IEEE/CVF International Conference on Computer Vision (ICCV)*, 2023, pp. 22189–22199.
- [13] Zhengyi Wang, Cheng Lu, Yikai Wang, Fan Bao, Chongxuan Li, Hang Su, and Jun Zhu, "Prolifedreamer: High-fidelity and diverse text-to-3d generation with variational score distillation," in *Advances in Neural Information Processing Systems (NeurIPS)*, 2023.
- [14] Fangzhou Hong, Mingyuan Zhang, Liang Pan, Zhongang Cai, Lei Yang, and Ziwei Liu, "Avatarclip: zero-shot text-driven generation and animation of 3d avatars," *ACM Trans. Graph.*, vol. 41, no. 4, July 2022.
- [15] Ruixiang Jiang, Can Wang, Jingbo Zhang, Menglei Chai, Mingming He, Dongdong Chen, and Jing Liao, "Avatarcraft: Transforming text into neural human avatars with parameterized shape and pose control," in *2023 IEEE/CVF International Conference on Computer Vision (ICCV)*, 2023, pp. 14325–14336.
- [16] Yukang Cao, Yan-Pei Cao, Kai Han, Ying Shan, and Kwan-Yee K. Wong, "Dreamavatar: Text-and-shape guided 3d human avatar generation via diffusion models," in *2024 IEEE/CVF Conference on Computer Vision and Pattern Recognition (CVPR)*, 2024, pp. 958–968.
- [17] Ye Yuan, Xueting Li, Yangyi Huang, Shalini De Mello, Koki Nagano, Jan Kautz, and Umar Iqbal, "Gavatar: Animatable 3d gaussian avatars

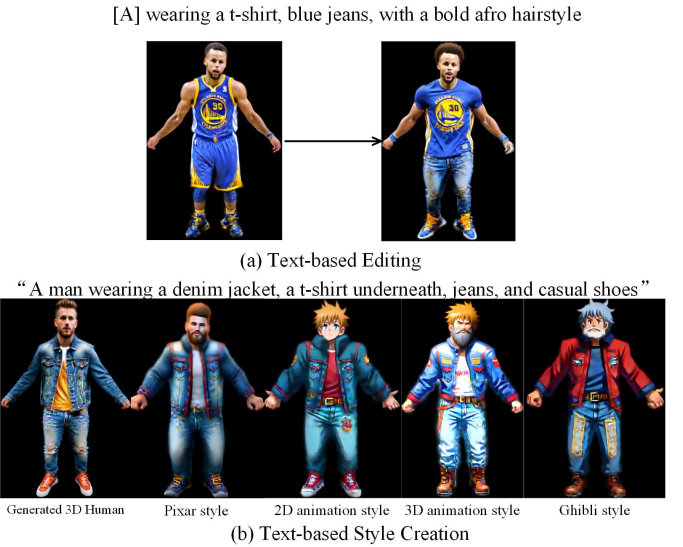


Fig. 5. Applications of our method.

“A man wearing a graphic tee featuring a retro gaming design, slim-fit jeans, blue sneakers, and a thick-rimmed glasses”



“A sturdy elderly man wearing khaki pants, black hiking boots, a olive green down jacket”



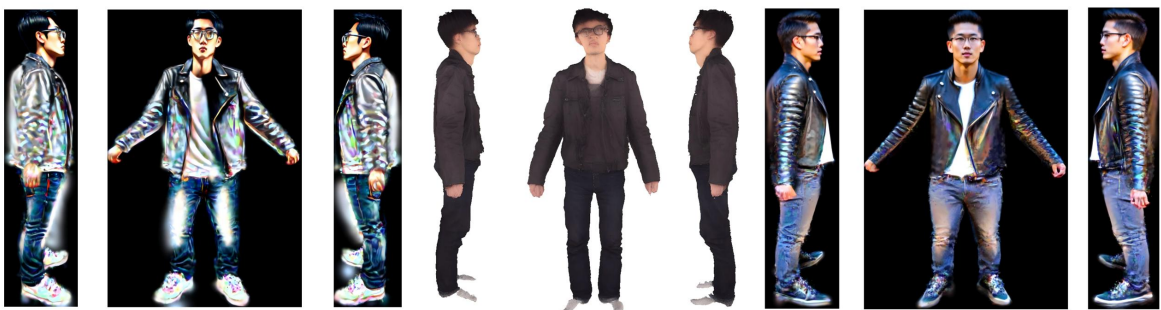
“An elderly European woman wearing a deep red wool scarf, brown knee-high boots, a wool coat, and thin-framed glasses”



“A white man wearing denim jeans, work boots, a navy blue wool sweater, a brown wide-brimmed hat, and black sunglasses”



“An Asian wearing dark jeans, white t-shirt, a black leather jacket, and glasses”



HumanGaussian

HumanNorm

Ours

Fig. 6. Qualitative comparisons with the SOTA methods.

with implicit mesh learning,” in *2024 IEEE/CVF Conference on Computer Vision and Pattern Recognition (CVPR)*, 2024, pp. 896–905.

[18] Yuze Wang, Junyi Wang, and Yue Qi, “We-gs: An in-the-wild efficient 3d gaussian representation for unconstrained photo collections,” 2024.

[19] Luping Liu, Chao Du, Tianyu Pang, Zehan Wang, Chongxuan L, and Dong Xu, “Improving long-text alignment for text-to-image diffusion models,” *arXiv preprint arXiv:2410.11817*, 2024.